
Efficient Distributed Auto-Differentiation

Bradley T. Baker¹ Vince D. Calhoun¹ Barak A. Pearlmutter² Sergey M. Plis¹

Abstract

Although distributed machine learning has opened up numerous frontiers of research, the separation of large models across different devices, nodes, and sites can invite significant communication overhead, making reliable training difficult. The focus on gradients as the primary shared statistic during training has led to a number of intuitive algorithms for distributed deep learning; however, gradient-based algorithms for training large deep neural networks (DNNs) are communication-heavy, often requiring additional modifications via sparsity constraints, compression, quantization, and other similar approaches, to lower bandwidth. We introduce a surprisingly simple statistic for training distributed DNNs that is more communication-friendly than the gradient. The error backpropagation process can be modified to share these smaller intermediate values instead of the gradient, reducing communication overhead with no impact on accuracy. The process provides the flexibility of averaging gradients during backpropagation, enabling novel flexible training schemas while leaving room for further bandwidth reduction via existing gradient compression methods. Finally, consideration of the matrices used to compute the gradient inspires a new approach to compression via structured power iterations, which can not only reduce bandwidth but also enable introspection into distributed training dynamics, without significant performance loss.

1. Introduction

Deep Neural Networks (DNNs) are machine learning models capable of detecting complex nonlinear patterns in data which other simpler models may struggle to detect. In exchange, the large number of parameters at work in DNNs require significant amounts of data to train, with over-fitting becoming a real possibility if not enough data are provided, or the network is not otherwise regularized. The need for training on large amounts of data in reasonable time has turned the focus of deep learning community to the so called data-parallel training where models on different (GPU) processors are synchronously trained on their respective subsets of data (Shallue et al., 2019) maintaining the same gradient. This approach was further scaled to solutions in which DNNs are trained in a distributed network of data-collection sites, intermittently sharing statistics during training so that local models are soon able to learn global trends in the data (Cano et al., 2016).

Distributed deep learning can also be motivated by a desire to keep local training samples hidden. For example, the application of deep learning to medical problems which utilize highly personal data such as medical imaging scans or DNA sequences can require models to be trained on samples which cannot be transferred from one data gathering site to another due to legal or ethical considerations. These issues motivate privacy-sensitive toolboxes for distributed learning, such as COINSTAC (Plis et al., 2016).

Distributed deep learning has been dominated by distributed stochastic gradient descent (dSGD) (Bottou, 2010; Verbraeken et al., 2020), a generic and intuitive method for distributed convex optimization in which gradients computed at local sites are periodically aggregated and broadcast back to local sites. With these aggregated gradients, each local site can update their model as if it had seen the data on other sites. The linearity of the gradient and its utility for optimization make its use in distributed algorithms both intuitive and, generally, correct. It turns out, however, that distributed deep learning is founded on more than gradients alone.

¹Tri-Institutional Center for Translational Research in Neuroimaging and Data Science {Georgia State University, Georgia Institute of Technology, Emory University }, Atlanta, Georgia ²Dept. of Computer Science, Maynooth University, Maynooth, Ireland. Correspondence to: Bradley Baker <bbaker43@gsu.edu>.

In this work, we examine distributed deep learning via the mechanism of reverse-mode automatic differentiation, or Reverse AD (Speelpenning, 1980). We find that the constituent matrices gathered during the forward and backward passes of reverse AD, which are used to compute the gradients, can be transferred instead, yielding a substantial saving in bandwidth over standard dSGD. Furthermore, we can use the structure of the outer product used to compute the gradient to provide an efficient low-rank approximation of the gradient using only low-rank versions of these constituent matrices. These low rank approximations also provide “free” introspection into the training dynamics of the distributed network, due to their structural relationship to the gradient. There is more to distributed training than gradients, and by examining these other pieces, we gain not only a more efficient algorithm, but also insight into the black box of deep learning.

2. Related Work

Most relevant work in distributed deep learning focuses on gradients as the primary shared statistic, and applies techniques such as dropping unnecessary values via sparsification (Aji & Heafield, 2017; Wang et al., 2018; Stich, 2018; Wen et al., 2017; Sattler et al., 2019a;b; Shi et al., 2019), mapping values into bins via quantization (Alistarh et al., 2016; Agarwal et al., 2018; Bernstein et al., 2018; Horváth et al., 2019; Yu et al., 2018), or otherwise compressing gradients (Lin et al., 2017; Koloskova et al., 2019; Mishchenko et al., 2019). Although these methods focus on gradients, the majority of them are applicable to any shared statistic which can be used for learning. Since we focus on the more fundamental question of what statistics are being shared, these methods are potentially synergistic with ours.

A second class of distributed deep learning method reduces bandwidth by following an update schedule, so gradients are not shared for every batch or epoch. These methods, such as bursty aggregation (Zhang et al., 2017), lazy aggregation (Chen et al., 2018), periodic averaging (Haddadpour et al., 2019), and other scheduling strategies (Stich, 2018; Yu et al., 2019; Assran et al., 2019), are again agnostic to the actual statistic shared—so long as the statistic can be used for learning. With the exception of methods which average statistics during training, the methods proposed here should be entirely compatible with any update schedule desired, since the auto-differentiation statistics we share can be used to reconstruct gradients at any point during training.

The method most closely related to that proposed here is PowerSGD (Vogels et al., 2019), which uses a QR decomposition of local gradients to estimate two low-rank matrices which can be used to reconstruct a low-rank approximation of the gradient. Although PowerSGD is a gradient compression method on its face, the sharing of low-rank Q and R matrices does represent a shift away from sharing raw gradients. Indeed, for a chosen low rank r , PowerSGD is able to achieve a bandwidth per layer of $\Theta(r(h_i + h_{i+1}))$ for hidden layer sizes h_i and h_{i+1} . PowerSGD thus represents a competitor to our method which arrived at a bandwidth reduction via the path of QR decomposition rather than Auto-Differentiation. It will be our goal in this work to illustrate the benefits we receive by taking the path of auto-differentiation both in terms of mathematical intuition, model performance, and bandwidth reduction.

3. Methods

Let $\mathcal{N}(W)$ be a deep neural network with L hidden layers. Let $\mathbf{X} \in \mathbb{R}^{N \times M}$ be the input batch of data with N samples and M dimensions. Let $\mathbf{Y} \in \mathbb{R}^{N \times C}$ be the target variable of dimension with N samples and C dimensions. let h_i be the size of the i th hidden layer. For a feed-forward network, the weight matrices are thus $\mathbf{W}_i \in \mathbb{R}^{h_i \times h_{i+1}}$, with $h_0 = M$ and $h_{L+1} = C$. Let $\varphi_i(x)$ be the activation used at layer i in the network, and let \mathcal{L} be a given cost-function.

For a feed-forward network, the activations at layer i are thus computed as

$$\mathbf{Z}_i = \mathbf{A}_{i-1} \mathbf{W}_i + \mathbf{B}_i \quad (1a)$$

$$\mathbf{A}_i = \varphi_i(\mathbf{Z}_i) \quad (1b)$$

3.1. Reverse-Mode Auto-Differentiation

AD is a class of methods through which derivatives of functions may be calculated during the execution of a code which evaluates that function. The backpropagation algorithm for training deep neural networks is specific case of *reverse-mode* AD, in which derivatives are propagated *backwards* along the data flow graph. This is a two stage process: first a *forward pass* through the function is computed, during which intermediate outputs from expressions within the function are saved and relationships between variables are recorded. After the forward pass, a *backward pass* evaluates the contribution of each intermediate variable to the derivative of the output, retracing and combining intermediate variables and expressions until

we return to the input. (For a survey, see [Baydin et al., 2018](#)).

Following reverse mode AD, we use the chain rule to compute the derivative at each layer. At the output layer, we first compute the gradient of the loss w.r.t. the output activations $\nabla_{\mathbf{A}_L} \mathcal{L}$, and take the Hadamard product with the derivative at the output activation $\varphi'_L(\mathbf{Z}_L)$ to compute the gradient w.r.t. the output, i.e., Δ_L

$$\Delta_L = \nabla_{\mathbf{A}_L} \mathcal{L} \odot \varphi'_L(\mathbf{Z}_L) \quad (2)$$

At higher layers (where $i < L$), we can continue to compute these errors as

$$\Delta_i = (\Delta_{i+1} \mathbf{W}_i \odot \varphi'_i(\mathbf{Z}_i)) \quad (3)$$

At layer i , the gradient of the weights $\nabla_{\mathbf{W}_i} \mathcal{L}$ at layer i can thus be computed exactly as

$$\nabla_{\mathbf{W}_i} \mathcal{L} = \mathbf{A}_{i-1}^\top \Delta_i \quad (4)$$

The key insight offered to us by the reverse-mode AD perspective into deep learning is that in many cases the dimensionality of the intermediate variables accumulated during the forward and backwards passes of AD will be less than that of the gradient. In other words, the gradient is a low rank matrix in most practically relevant cases, and this rank is limited from above by the batch size. For example, consider a matrix-vector product $y = Wx$. If Alice is transmitting the gradient $\nabla_W \mathcal{L}$ to Bob, where only Alice knows x , we can note that $\nabla_W \mathcal{L}$ is the outer product of x and $\nabla_y \mathcal{L}$. If $W \in \mathbb{R}^{m \times n}$, then these two vectors together have dimensionality $m + n$, and we are often in the regime where $m + n \ll m \times n$.

This observation suggests a novel algorithm for backpropagation via distributed auto-differentiation (dAD). We will present this algorithm and some more communication-efficient variants in the following sections.

3.2. Distributed Auto-Differentiation (dAD)

As a first step, we propose a distributed algorithm named ‘‘Distributed Auto-Differentiation’’ which exploits the structure of the auto-differentiation algorithm so that the total bandwidth passed for each batch from local sites to the aggregator is $\Theta(N \sum_{i=0}^{L+1} h_i)$, and the bandwidth passed from aggregator to the local sites is $\Theta(SN \sum_{i=0}^{L+1} h_i)$. In contrast to the efficient method described below, this method allows for the *exact* computation of global gradients.

Rather than transmitting statistics after the backpropagation algorithm has already computed gradients, as is usual in federated learning, we transmit statistics once for each layer.

First, at the output layer on each local site, we compute Δ_L . Then \mathbf{A}_{L-1} and Δ_L are sent to the aggregator, consuming a bandwidth of exactly $N(h_L + C)$.

At the aggregator, we then compute $\hat{\mathbf{A}}_{L-1} \in \mathbb{R}^{SN \times h_L}$, and $\hat{\Delta}_L \in \mathbb{R}^{SN \times C}$ by concatenating the received statistics in their batch dimension. These are then both broadcast back to each of the local sites for a further bandwidth cost of $SN(2h_L + C)$.

At each local site, the gradient can now be computed as in equation 4 by just substituting the aggregated values, $\hat{\Delta}_L$ and $\hat{\mathbf{A}}_{L-1}$ for Δ_L and \mathbf{A}_{L-1} respectively. The procedure can be iteratively performed for each layer encountered during backpropagation, allowing each site to compute an exact copy of the global gradients for a communication of $\Theta(N(h_i + h_{i+1}))$ from the local sites, and a communication of $\Theta(SN(h_i + h_{i+1}))$ from the aggregator.

3.3. Efficient dAD

This section presents a more communication-efficient version of dAD called *efficient dAD*, or edAD. This method illustrates how the structure of auto-differentiation can be exploited to provide further benefits in terms of bandwidth reduction without sacrificing analytical correctness.

Distributed auto-differentiation as presented above for deep neural networks is quite naïve; however, just switching our focus from sharing gradients to sharing the statistics used for AD has already provided a communication benefit over standard distributed SGD, while still preserving exact gradient computations. We propose a further extension of distributed Auto-Differentiation, which we call efficient auto-differentiation (edAD), which further reduces communication while still allowing for exact gradient computation.

Algorithm 1 distributed auto-differentiation (dAD)

```

1: procedure DAD( $\{\mathcal{N}_s\}_s^S, \{\mathbf{X}_s\}_s^S, \{\mathbf{Y}_s\}_s^S$ )
2:   for site  $s$  do
3:      $\{\mathbf{A}_i^{(s)}\}_{i=0}^L = \text{forward}(\mathcal{N}_s, \mathbf{X}_s)$ 
4:   end for
5:   for hidden layer  $i = L, 0 < i \leq L$  do
6:     for site  $s$  do
7:       if  $i == L$  then
8:          $\Delta_L^{(s)} = \nabla_{\mathbf{A}_L} \mathcal{L} \odot \varphi'(\mathbf{Z}_L^{(s)})$ 
9:       else
10:         $\Delta_i^{(s)} = \Delta_{i+1}^{(s)} \mathbf{W}_i^{(s)} \odot \varphi'_i(\mathbf{Z}_i^{(s)})$ 
11:      end if
12:       $\text{sendToAggregator}(\mathbf{A}_{i-1}^{(s)}, \Delta_i^{(s)})$ 
13:    end for
14:     $\hat{\Delta}_i = \text{vertcat}(\{\Delta_i^{(s)}\}_s^S)$  ▷ At Aggregator
15:     $\hat{\mathbf{A}}_{i-1} = \text{vertcat}(\{\mathbf{A}_{i-1}^{(s)}\}_s^S)$  ▷ At Aggregator
16:     $\text{broadcastToSites}(\hat{\mathbf{A}}_{i-1}, \hat{\Delta}_i)$ 
17:    for site  $s$  do
18:       $\nabla_{\mathbf{W}_i}^{(s)} = \hat{\mathbf{A}}_{i-1}^\top \hat{\Delta}_i$ 
19:    end for
20:  end for
21: end procedure

```

The efficient version of dAD begins in much the same way as before, with computation and sharing of exact gradients and activations at the output layer. We notice, however, in equation 3, that the updated deltas computed at each iteration only depend on the previously computed deltas, and the derivative of the activation function w.r.t. the output activations at a given layer. Indeed, for most common classes of activation function, if we know only the output activations, we can compute the derivative analytically, provided we know the activation function used at that layer. Since we are already accumulating the input activations at each step in our algorithm, these can be reused as the output activations at the next layer. Thus, the Δ_i values can just be updated locally without any additional communication, effectively reducing the cost of communication by half.

As we continue iteratively through hidden layers in the backpropagation algorithm, we compute the updates to local Δ_i values using the aggregated $\hat{\Delta}_i$ values. Note that because these values only depend on previous deltas and activations, we do not need to continue sending Δ values, as long as the received aggregated $\hat{\Delta}_L$ values are used for these computations. Namely, we compute for each subsequent layer

$$\hat{\Delta}_i = \hat{\Delta}_{i+1} \mathbf{W}_i^\top \odot \hat{\mathbf{A}}'_i \quad (5)$$

where $\hat{\mathbf{A}}'_i$ is the derivative of the output layer i , computed using only the known output activations.

Thus, using this algorithm for distributed auto-differentiation, we can compute the exact gradient values for the aggregate model with only $\Theta(Nh_i)$ sent from local sites, and $\Theta(SNh_i)$ from the aggregator.

3.4. Rank-reduced dAD

We have shown that taking advantage of the low-rank outer product structure of the gradient in reverse-mode AD allows computing exact gradients with a free bandwidth reduction over dSGD (dAD) that can be reduced further with the help of the structure of AD (edAD). If exact gradients are required, no further bandwidth reduction is possible under the current framework; however, the low-rank outer product structure of the gradient can be additionally exploited for efficiently reducing the rank further to r and instead of Δ_i and \mathbf{A}_i transferring smaller approximation matrices of no more than $r \ll N$ rows. We exploit that structure in computing power iterations that we use in the peeling method below. This is uniquely available to our method because we operate at the level AD rather than solving the problem when the gradient has already been computed.

Algorithm 2 efficient dAD (edAD)

```

1: procedure EDAD( $\{\mathcal{N}_s\}_s^S, \{\mathbf{X}_s\}_s^S, \{\mathbf{Y}_s\}_s^S$ )
2:   for site  $s$  do
3:      $\{\mathbf{A}_i^{(s)}\}_{i=0}^L = \text{forward}(\mathcal{N}_s, \mathbf{X}_s)$ 
4:   end for
5:   for hidden layer  $i = L, 0 < i \leq L$  do
6:     for site  $s$  do
7:       if  $i == L$  then
8:          $\Delta_L^{(s)} = \nabla_{\mathbf{A}_L} \mathcal{L} \odot \varphi'(\mathbf{Z}_L^{(s)})$ 
9:          $\text{sendToAggregator}(\mathbf{A}_{i-1}^{(s)}, \Delta_i^{(s)})$ 
10:      else
11:         $\hat{\Delta}_i^{(s)} = \hat{\Delta}_{i+1}^{(s)} \mathbf{W}_i^{(s)} \odot \hat{\mathbf{A}}_i'^{(s)}$ 
12:      end if
13:       $\text{sendToAggregator}(\mathbf{A}_{i-1}^{(s)})$ 
14:    end for
15:    if  $i == L$  then
16:       $\hat{\Delta}_L = \text{vercat}(\{\Delta_L^{(s)}\}_s^S)$  ▷ At Aggregator
17:       $\text{broadcastToSites}(\hat{\Delta}_L)$ 
18:    end if
19:     $\hat{\mathbf{A}}_{i-1} = \text{vercat}(\{\mathbf{A}_{i-1}^{(s)}\}_s^S)$  ▷ At Aggregator
20:     $\text{broadcastToSites}(\hat{\mathbf{A}}_{i-1})$ 
21:    for site  $s$  do
22:       $\nabla_{\mathbf{W}_i}^{(s)} = \hat{\mathbf{A}}_{i-1}^\top \hat{\Delta}_i$ 
23:    end for
24:  end for
25: end procedure

```

3.4.1. STRUCTURED POWER ITERATIONS

Observe that we can compute the singular vector corresponding to the dominant singular value of $\nabla_{\mathbf{W}_i} \mathcal{L}$ by iterating the following recurrence:

$$\mathbf{g}_{k+1}^1 = (\nabla_{\mathbf{W}_i} \mathcal{L})^\top (\nabla_{\mathbf{W}_i} \mathcal{L}) \mathbf{g}_k^1 \quad (6)$$

Relying on (4), and pre-computing $\mathbf{C} = \mathbf{A}_{i-1} \mathbf{A}_{i-1}^\top$, $\mathbf{B} = \Delta_i^\top \mathbf{C}$, we can instead iterate:

$$\mathbf{g}_{k+1}^1 = \mathbf{B} (\Delta_i \mathbf{g}_k^1) \quad (7)$$

Compared to the $O(h^2)$ complexity of the iteration (6), the complexity of the structured power iteration is just $O(h \times N)$ and since $N \ll h$ for all practical models, it is linear in h . The corresponding singular value $\sigma^1 = \sqrt{\mathbf{v}^\top \mathbf{C} \mathbf{v}}$ (where $\mathbf{v} = \Delta_i \mathbf{g}$) is computed in $O(h \times N)$ once per singular vector, while computation of the left singular vector \mathbf{q}^1 is just $O(h \times N)$ as $\mathbf{q}^1 = \mathbf{A}_{i-1}^\top \mathbf{v} / \sigma^1$.

We successively collect $(\sigma^j \mathbf{b}^j, \mathbf{c}^j)$, absorbing singular values into one of the vectors constructing respective \mathbf{G}_j and \mathbf{Q}_j by concatenating \mathbf{g} s and \mathbf{q} s as columns, and proceed to computing the next singular vectors set by peeling the previously computed least-squares optimal low-rank representation:

$$\begin{aligned} \mathbf{g}_{k+1}^j &= ((\nabla_{\mathbf{W}_i} \mathcal{L})^\top (\nabla_{\mathbf{W}_i} \mathcal{L}) - \mathbf{Q}_{j-1} \mathbf{G}_{j-1}^\top) \mathbf{g}_k^j \\ &= (\nabla_{\mathbf{W}_i} \mathcal{L})^\top (\nabla_{\mathbf{W}_i} \mathcal{L}) \mathbf{g}_k^j - \mathbf{Q}_{j-1} (\mathbf{G}_{j-1}^\top \mathbf{g}_k^j) \end{aligned} \quad (8)$$

We have already shown that complexity of the first component of (8) is linear in h , but the second component is clearly linear in h as well. Thus, thanks to the outer-product structure of AD gradients, we can compute low rank approximation in time linear in the layer width h .¹

¹To declutter notation we have dropped the layer index on h , as each $h \gg N$.

Manufacturer	Cores	Memory	GPUs
AMD	64	512 GB	1×Nvidia 2080
Nvidia DGX-1	40	512 GB	8×Nvidia V100
Dell	40	192 GB	4×Nvidia V100

Table 1. Specs for the SLURM cluster at GSU used to run the experiments described in §4.

We have additionally observed, that during training the true rank of $\nabla_{\mathbf{W}_i} \mathcal{L}$ fluctuates and although always below N may take significantly lower values than the desired r we pick for the structured power iterations. To skip computing noisy columns for our \mathbf{Q} and \mathbf{G} matrices, we stop the process when $\|\mathbf{g}^j - \mathbf{g}^{j+1}\|_2 / \|\mathbf{g}^j\|_2 < \theta$, where we set the threshold θ to 10^{-3} .

3.5. Application to Recurrent Networks

Since all of our methods are built from the standpoint of auto-differentiation, the application of dAD, edAD, and rank-dAD to recurrent networks is straightforward. When given a recurrent network, we unroll the recursion along the sequence, computing the forward pass as normal in AD. For the backward pass, we proceed as with feed-forward networks when applying dAD and edAD; however, we now transfer one set of activations and deltas per element in the sequence. Alternatively, we can accumulate over the entire unrolled network, and transfer the full activations and deltas over time. Provided that $TN \ll h_i$, this will still provide a reduction over standard dSGD.

For rank-dAD, on the other hand, recall that we can use power iterations to find B and C which are low rank, and approximate the full gradient averaged over batches and time. Thus, we can simply stack the local activations and deltas in the batch and time dimensions, and compute the low rank approximation of the resulting outer product which would otherwise be used to compute the gradient. This means for rank-dAD we can still obtain $O(r \times h_i)$ communication without having to perform additional transmissions.

3.6. Distributed Network Topology

For simplicity, for all methods presented herein we assume a star network topology, in which several sites with local data sets send statistics to a single trusted aggregator; however, all of the methods presented below could be ameliorated to peer-to-peer communication, where each local site can serve as an aggregator for what is received from other peers.

4. Results

This section presents the results of several experiments which illustrate the benefits of dAD, edAD, and rank-dAD. All experiments were run on a SLURM cluster at GSU which submits jobs to one of the 26 machines on the same network. Specs for these machines are provided in Table 1.

For all experiments, all networks were implemented in PyTorch 1.7.1 with Python 3.8 using an Adam optimizer with a fixed learning rate of 10^{-4} and batch size of 32 per site. In all scenarios, we tested with two distributed sites (except for pooled, which has one) which had the same architecture, and which initialized their weights with the same random seed. We performed $k = 5$ -fold cross-validation for all experiments, and plot the average results with error bars across these folds.

4.1. Equivalence of dAD and edAD to full SGD

We claimed above that dAD and edAD are equivalent methods to standard gradient descent and to distributed gradient descent. Although it is clear from our methods that this should be the case, we perform several small experiments to illustrate both the equivalence of dAD and edAD to the pooled case and the benefits of distributed learning.

4.1.1. FEED-FORWARD NETWORKS

As a first baseline, we begin with a simple demonstration of equivalence using a fully-connected network on the MNIST data set (LeCun et al., 1998). For the distributed setting, however, we complicate the standard digit-recognition task by allocating training samples to sites so that no one class can be found on more than one site. This is meant to emulate a difficult case in distributed learning, when the underlying distribution of labels or data on different sites are completely separate.

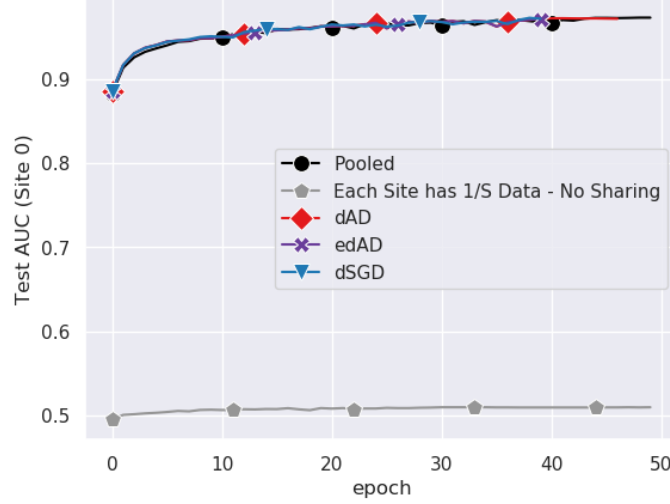


Figure 1. For a Feed-Forward network trained on the MNIST task, we show that the performance for dAD and edAD is equivalent to that of the pooled and dSGD versions of backpropagation, even when labels are separated onto different sites in the network.

Output Layer	size = 1024×10
dSGD	3.092×10^{-7}
dAD	3.035×10^{-7}
edAD	3.035×10^{-7}
Fully-Connected 2	size = 1024×1024
dSGD	1.491×10^{-7}
dAD	1.460×10^{-7}
edAD	1.444×10^{-7}
Fully-Connected 1	size = 768×1024
dSGD	3.851×10^{-7}
dAD	3.690×10^{-7}
edAD	2.695×10^{-7}

Table 2. Here we show the maximum error for the gradients computed during one epoch of training with various distributed methods, and with the pooled data all on one site.

The network implemented has two, fully-connected hidden layers with 1024 neurons at each layer. We train the distributed network for 50 epochs, and compare the AUC for each local model on a test data set which has all labels. The AUC trajectory for the training period is shown in Figure 1. Additionally, we measure the maximum error between the pooled and distributed gradients over the training period and provide the results below in Table 2.

4.1.2. RECURRENT NETWORKS

Next, we study the equivalence of dAD and edAD to the pooled case when applied to recurrent neural networks. We implement a recurrent network with a GRU cell which has a hidden dimension of 64. The GRU feeds into a fully-connected classifier with two hidden layers of width 512 and 256, respectively. As before, we test with two distributed sites.

We test our method on several data sets from the UEA multivariate time series classification archive (Bagnall et al., 2018), namely the Spoken Arabic Digits data set, the PIMS-SF data set, the NATOPS data set, and the PenDigits data set. In Figure 2 we compare the average test AUC for the Spoken Arabic Digits data set. As with the MNIST evaluation before, we elect to split labels across sites to illustrate the benefits of distributed learning for an extreme problem case.

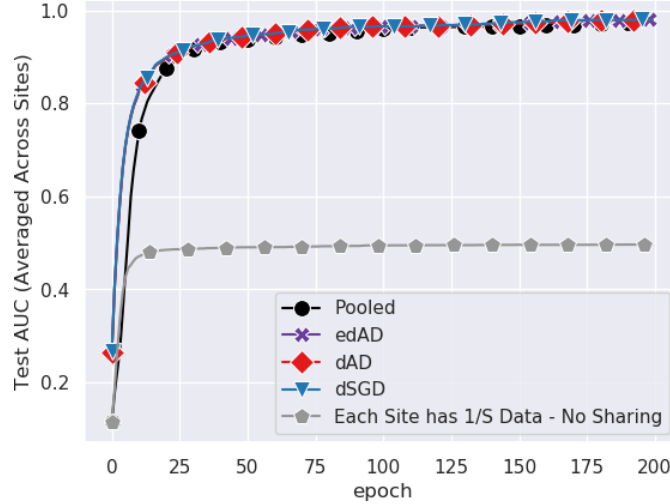


Figure 2. For a RNN with a GRU layer on the Spoken Arabic Digits data set we show that the performance for dAD and edAD is equivalent to pooled and dSGD backpropagation.

4.2. Rank-dAD

This section presents results which illustrate the benefits of rank-dAD. For testing purposes, we keep the number of iterations used by rank-dAD set to 10, so that we are sure that the number is always much smaller than the hidden layer size. For comparison, we reimplemented PowerSGD from scratch following the description in Vogels et al. 2019, and by consulting the github repository for that paper, which includes source code. For both rank-dAD and PowerSGD, we tested both the MNIST and UEA data sets with the same Feed-Forward and Recurrent network tested previously.

4.2.1. PERFORMANCE COMPARISON

First, we compare the performance of PowerSGD and rank-dAD for increasing rank. In Figure 3, we plot the average test AUC during the training period for both MNIST and the Spoken Arabic Digits data set. The plots for the remaining UEA data sets are located in the appendix. Above rank 3, the performance of both algorithms is more-or-less equivalent on both data sets, with our method winning slightly for the Spoken Arabic Digits data set.

4.2.2. EFFECTIVE RANK IN RANK-DAD

As shown above, our focus on auto-differentiation gives us a unique perspective into low-rank reductions via structured power iterations. This section presents initial empirical results studying how our method is able to dynamically estimate the rank of gradients during training, both lowering bandwidth and providing unique insight into the training dynamics of the networks we study here.

We call the rank estimated using the structured power-iterations (§3.4.1) the *effective rank* of the gradient, and during training we measure the rank computed at each layer in the network for each batch. At each epoch we compute the average effective rank over all the batches for that epoch, and plot that effective rank over the training period. To make sure we get a strong characteristic of the actual rank of the matrices, we set the maximum rank to 32, which is the batch size, and thus the upper-limit of the actual rank for the gradients.

Figure 4 shows how the effective rank of a feed-forward network’s gradients change during 50 training epochs on the MNIST data set, with the curve for each layer plotted separately. Figure 5 shows the effective rank of a recurrent network with a GRU cell for several UEA data sets, over a training period of 100 epochs. In each plot, the GRU input-to-hidden layer, the GRU hidden-to-hidden layer, and the first fully-connected layer, the second fully-connected layer, and the output layer are plotted separately.

5. Discussion

This section presents an analysis of the theoretical and empirical results provided above, taking note of how each result contributes to support our claims.

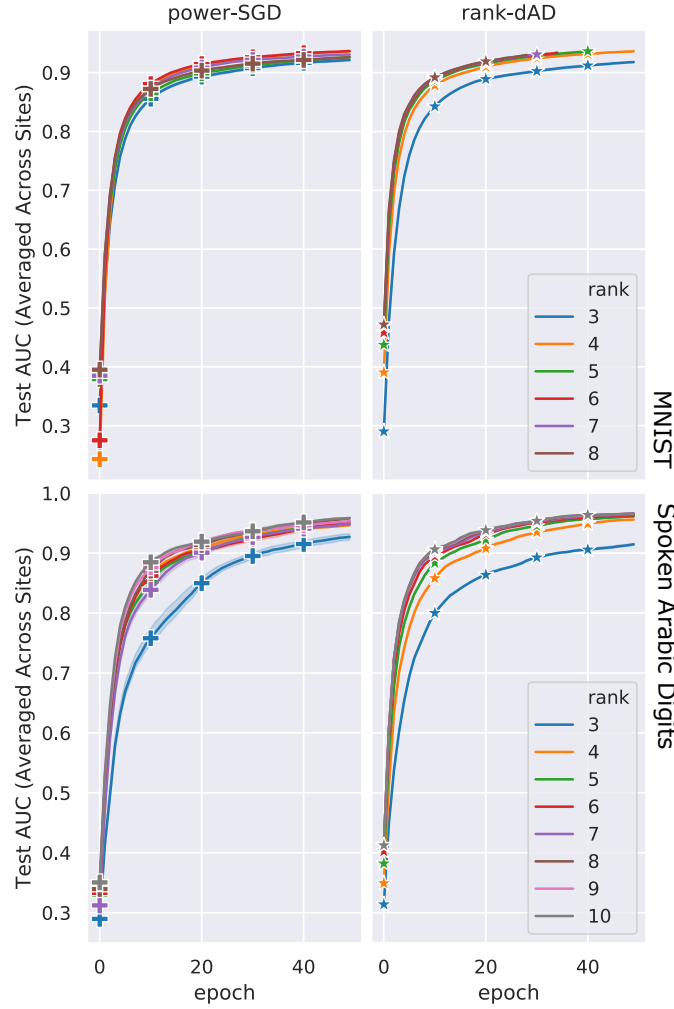


Figure 3. The average test AUC across sites for power-SGD and rank-dAD with increasing rank. The top panel shows the AUC over 50 epochs for the MNIST data set, and the bottom panel shows the AUC for the Spoken Arabic Digits data set.

5.1. Performance

Because dAD and edAD involve the transmission of full activations and deltas to all sites, the gradients computed by both methods exactly match those which would be computed in the pooled case, or in distributed SGD. See Figures 1 and 2 for an empirical verification of this claim.

For different initial ranks, our algorithm performs on par with PowerSGD on MNIST, and often better on the UEA data sets (see Figures 3 and 5). We attribute our improved performance over PowerSGD to a stronger robustness of our low-rank approximation of the gradient in the L_2 sense.

5.2. Analysis of Effective Rank

In Figure 4, we provide a plot of the effective gradient rank estimated by our structured power iterations method during training. Even though the maximum rank was set to 10, the power iterations on average detect a smaller underlying rank in the gradient. Additionally, we observe that the statistics computed at the output layer always has a smaller rank than the other two fully-connected layers in the network. At all layers, the rank of the computed statistics decreases during training, which seems to correspond to the model’s improved performance.

The effective rank as measured for the GRU network in Figure 5 provide a similarly intriguing story. Over all data sets, the Output layer at the GRU has a much smaller rank than the initially chosen maximum rank, and for three of the data sets, the output layer provides statistics with a rank lower than all other layers, consistent with the results seen for the MNIST data.

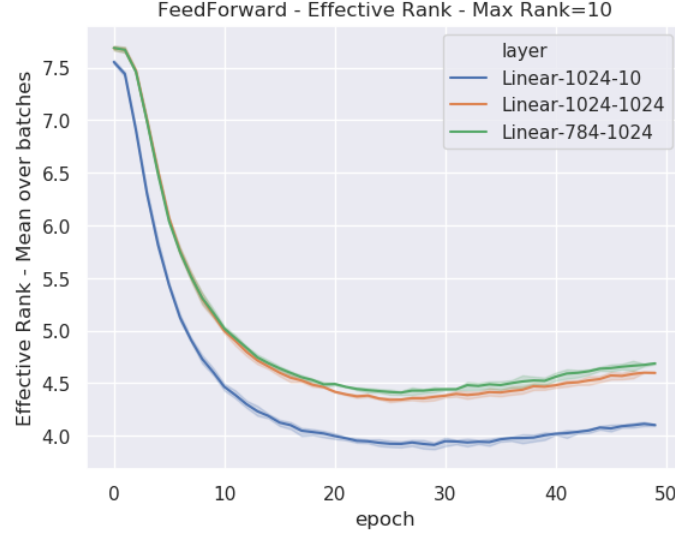


Figure 4. Effective rank for the MNIST data set, where the initial maximum rank was set to 10. For each batch, local power iterations were computed prior to transmitting statistics, and the actual rank estimated was then measured. The green curve shows the average effective rank of the gradients as computed at the input layer, the orange curve shows the next fully connected layer, and the blue curve shows the output layer.

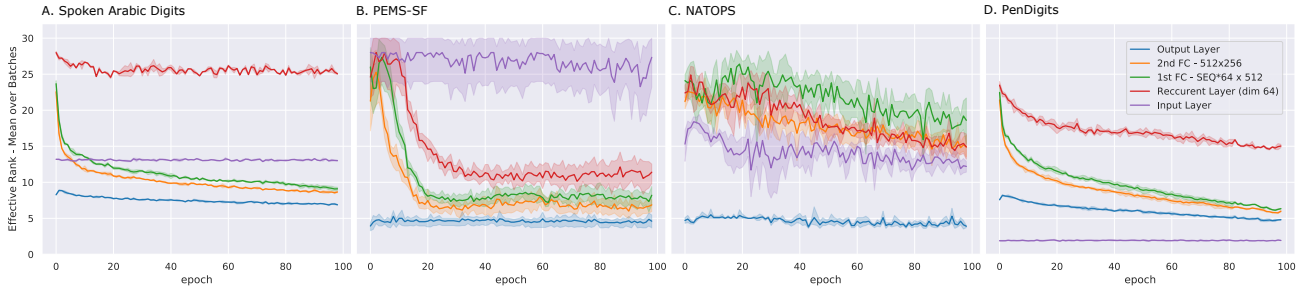


Figure 5. Effective Rank computed using structured power iterations during training for a GRU trained over 100 epochs for several data sets. In each plot, the GRU input layer is plotted in purple, the recurrent layer in red, the first fully-connected classification layer in green, the second fully-connected classification layer in orange, and the output layer is plotted in blue.

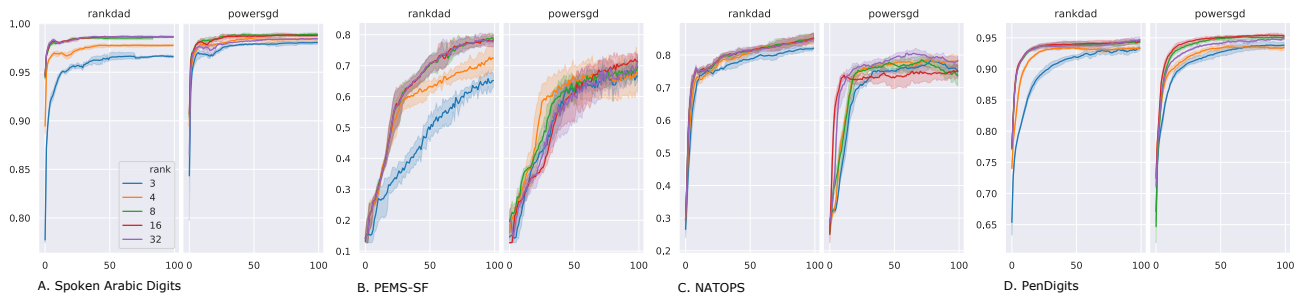


Figure 6. The test AUC for a GRU trained with rank-dAD compared with the same architecture trained with PowerSGD. Each curve in the two plots provides the AUC over training for a different maximum rank.

All four of the tested data sets for the GRU also show a clear decrease in rank during training for both of the Fully-Connected layers in the classifier part of the network (consistently with MNIST). For three of the data sets tested, the input layer shows an effective rank much lower than the maximum chosen rank; however, only the NATOPS data set indicates that the rank of statistics computed at this layer decreases in any noticeable way during the training period. On the other hand, the recurrent layer in all networks does see a decrease in the rank of its statistics during training, though the decrease tends to be much less pronounced than in the classifier layers.

5.3. Future Work

The key insight of our work is that auto-differentiation provides a unique and useful perspective into distributed deep learning, which can be utilized both to improve the bandwidth of distributed algorithms and to examine the dynamics involved in learning.

5.3.1. EXTENSION TO GENERAL-PURPOSE AD

AD has applications to machine learning beyond deep learning, such as generic gradient-based optimization with the Hessian (Pearlmutter, 1994; Agarwal et al., 2017), or Bayesian posterior inference in MCMC (Meyer et al., 2003). Further work is required to look into auto-differentiation as a potentially distributable process in and of itself; however, such work would open up a much wider domain of machine learning to the insights provided here.

5.3.2. THE PROBLEM WITH CONVOLUTIONS

In their current form, dAD, edAD, and rank-dAD all share input activations for the given layers in the network. For feed-forward and recurrent networks (as well as transformers), the bandwidth improvements provided over dSGD are obvious. Convolutional layers, however, present a bandwidth problem for these methods, because the size of the resulting output activations from a convolutional layer tend to be much larger in size than the number of parameters within that layer. Thus, further work is needed in examining AD applied to convolutional layers to see if bandwidth reduction is available without the addition of heuristics.

5.3.3. EFFECTIVE GRADIENT RANK FOR INTROSPECTION AND DNN DYNAMICS

Although our initial approach was to use the unique structure provided to us by AD to compute an accurate low-rank approximation, the apparent dynamics this approach reveals beg for further empirical and theoretical analysis. The Singular Value Decomposition has been used to study the dynamics of training in networks with linear activations (Saxe et al., 2013), and it is possible that distributed models may be provided with such an analysis for free when using our method. By opening the black box of AD, we may get a peek into the black box of deep learning for free.

6. Conclusion

In this work, we took a step back from standard gradient-based methods for distributed deep learning, and presented a novel algorithm for distributed auto-differentiation (dAD). The insight that the intermediate outer product factors gathered by AD can be transferred instead of the full gradient already provides a significant bandwidth reduction over full-gradient methods like dSGD. Furthermore, we are able to show that the structure of AD can be further capitalized on to reduce bandwidth again by half, since for standard backpropagation, the global delta values can be back-propagated through the network as long as the activations are still shared. Finally, we push dAD even further by exploiting the explicit outer-product structure to obtain low rank approximations for the gradient in terms of low-rank versions of the intermediate statistics. With this, rank-dAD provides an intriguing method for adaptively reducing bandwidth where the chosen rank is an *upper*-limit on communication. We are also able to analyze how the effective rank of the gradient changes during training, and thus obtain introspective information about the learning dynamics. It has been our goal to illustrate that auto-differentiation provides a rich landscape for further exploration into distributed deep learning. The reduction in bandwidth, intuitive algorithms, and competitive performance we have demonstrated here represent the first of potentially many benefits available to distributed machine learning practice and theory.

Acknowledgements

This work was supported by NIH 1R01DA040487 and 2RF1MH121885.

References

- Agarwal, N., Bullins, B., and Hazan, E. Second-order stochastic optimization in linear time. *Journal of Machine Learning Research*, 18(116):1–40, 2017. Also arXiv:1602.03943.
- Agarwal, N., Suresh, A. T., Yu, F. X. X., Kumar, S., and McMahan, B. CPSGD: Communication-efficient and differentially-private distributed SGD. In *Advances in Neural Information Processing Systems*, pp. 7564–7575, 2018.
- Aji, A. F. and Heafield, K. Sparse communication for distributed gradient descent. *arXiv preprint arXiv:1704.05021*, 2017.
- Alistarh, D., Grubic, D., Li, J., Tomioka, R., and Vojnovic, M. QSGD: Communication-efficient SGD via gradient quantization and encoding. *arXiv preprint arXiv:1610.02132*, 2016.
- Assran, M., Loizou, N., Ballas, N., and Rabbat, M. Stochastic gradient push for distributed deep learning. In *International Conference on Machine Learning*, pp. 344–353. PMLR, 2019.
- Bagnall, A., Dau, H. A., Lines, J., Flynn, M., Large, J., Bostrom, A., Southam, P., and Keogh, E. The UEA multivariate time series classification archive, 2018. *arXiv preprint arXiv:1811.00075*, 2018.
- Baydin, A. G., Pearlmutter, B. A., Radul, A. A., and Siskind, J. M. Automatic differentiation in machine learning: A survey. *Journal of Machine Learning Research*, 18, 2018.
- Bernstein, J., Wang, Y.-X., Azizzadenesheli, K., and Anandkumar, A. signSGD: Compressed optimisation for non-convex problems. *arXiv preprint arXiv:1802.04434*, 2018.
- Bottou, L. Large-scale machine learning with stochastic gradient descent. In *Proceedings of COMPSTAT’2010*, pp. 177–186. Springer, 2010.
- Cano, I., Weimer, M., Mahajan, D., Curino, C., and Fumarola, G. M. Towards geo-distributed machine learning. *arXiv preprint arXiv:1603.09035*, 2016.
- Chen, T., Giannakis, G., Sun, T., and Yin, W. LAG: Lazily aggregated gradient for communication-efficient distributed learning. In *Advances in Neural Information Processing Systems*, pp. 5050–5060, 2018.
- Haddadpour, F., Kamani, M. M., Mahdavi, M., and Cadambe, V. Local SGD with periodic averaging: Tighter analysis and adaptive synchronization. In *Advances in Neural Information Processing Systems*, pp. 11082–11094, 2019.
- Horváth, S., Kovalev, D., Mishchenko, K., Stich, S., and Richtárik, P. Stochastic distributed learning with gradient quantization and variance reduction. *arXiv preprint arXiv:1904.05115*, 2019.
- Koloskova, A., Lin, T., Stich, S. U., and Jaggi, M. Decentralized deep learning with arbitrary communication compression. *arXiv preprint arXiv:1907.09356*, 2019.
- LeCun, Y., Bottou, L., Bengio, Y., and Haffner, P. Gradient-based learning applied to document recognition. *Proceedings of the IEEE*, 86(11):2278–2324, November 1998.
- Lin, Y., Han, S., Mao, H., Wang, Y., and Dally, W. J. Deep gradient compression: Reducing the communication bandwidth for distributed training. *arXiv preprint arXiv:1712.01887*, 2017.
- Meyer, R., Fournier, D. A., and Berg, A. Stochastic volatility: Bayesian computation using automatic differentiation and the extended Kalman filter. *The Econometrics Journal*, 6(2):408–420, 2003.
- Mishchenko, K., Gorbunov, E., Takáč, M., and Richtárik, P. Distributed learning with compressed gradient differences. *arXiv preprint arXiv:1901.09269*, 2019.
- Pearlmutter, B. A. Fast exact multiplication by the Hessian. *Neural computation*, 6(1):147–160, 1994.
- Plis, S. M., Sarwate, A. D., Wood, D., Dieringer, C., Landis, D., Reed, C., Panta, S. R., Turner, J. A., Shoemaker, J. M., Carter, K. W., et al. COINSTAC: a privacy enabled model and prototype for leveraging and processing decentralized brain imaging data. *Frontiers in neuroscience*, 10:365, 2016.
- Sattler, F., Wiedemann, S., Müller, K.-R., and Samek, W. Sparse binary compression: Towards distributed deep learning with minimal communication. In *2019 International Joint Conference on Neural Networks (IJCNN)*, pp. 1–8. IEEE, 2019a.
- Sattler, F., Wiedemann, S., Müller, K.-R., and Samek, W. Robust and communication-efficient federated learning from non-iid data. *IEEE transactions on neural networks and learning systems*, 2019b.
- Saxe, A. M., McClelland, J. L., and Ganguli, S. Exact solutions to the nonlinear dynamics of learning in deep linear neural

- networks. *arXiv preprint arXiv:1312.6120*, 2013.
- Shallue, C. J., Lee, J., Antognini, J., Sohl-Dickstein, J., Frostig, R., and Dahl, G. E. Measuring the effects of data parallelism on neural network training. *Journal of Machine Learning Research*, 20:1–49, 2019. URL <https://www.jmlr.org/papers/volume20/18-789/18-789.pdf>. Also arXiv:1811.03600v3.
- Shi, S., Wang, Q., Zhao, K., Tang, Z., Wang, Y., Huang, X., and Chu, X. A distributed synchronous SGD algorithm with global Top- k sparsification for low bandwidth networks. In *2019 IEEE 39th International Conference on Distributed Computing Systems (ICDCS)*, pp. 2238–2247. IEEE, 2019.
- Speelpenning, B. *Compiling Fast Partial Derivatives of Functions given by Algorithms*. PhD thesis, Department of Computer Science, University of Illinois at Urbana-Champaign, USA, 1980. AAI8017989.
- Stich, S. U. Local SGD converges fast and communicates little. *arXiv preprint arXiv:1805.09767*, 2018.
- Verbraeken, J., Wolting, M., Katzy, J., Kloppenburg, J., Verbelen, T., and Rellermeyer, J. S. A survey on distributed machine learning. *ACM Computing Surveys (CSUR)*, 53(2):1–33, 2020.
- Vogels, T., Karimireddy, S. P., and Jaggi, M. PowerSGD: Practical low-rank gradient compression for distributed optimization. *arXiv preprint arXiv:1905.13727*, 2019.
- Wang, H., Sievert, S., Liu, S., Charles, Z., Papailiopoulos, D., and Wright, S. Atomo: Communication-efficient learning via atomic sparsification. In *Advances in Neural Information Processing Systems*, pp. 9850–9861, 2018.
- Wen, W., Xu, C., Yan, F., Wu, C., Wang, Y., Chen, Y., and Li, H. Terngrad: Ternary gradients to reduce communication in distributed deep learning. In *Advances in neural information processing systems*, pp. 1509–1519, 2017.
- Yu, H., Yang, S., and Zhu, S. Parallel restarted SGD with faster convergence and less communication: Demystifying why model averaging works for deep learning. In *Proceedings of the AAAI Conference on Artificial Intelligence*, volume 33, pp. 5693–5700, 2019.
- Yu, M., Lin, Z., Narra, K., Li, S., Li, Y., Kim, N. S., Schwing, A., Annavaram, M., and Avestimehr, S. Gradiveq: Vector quantization for bandwidth-efficient gradient aggregation in distributed cnn training. In *Advances in Neural Information Processing Systems*, pp. 5123–5133, 2018.
- Zhang, H., Zheng, Z., Xu, S., Dai, W., Ho, Q., Liang, X., Hu, Z., Wei, J., Xie, P., and Xing, E. P. Poseidon: An efficient communication architecture for distributed deep learning on GPU clusters. In *2017 USENIX Annual Technical Conference (USENIX ATC 17)*, pp. 181–193, 2017.